PAPER

NJC
www.rsc.org/njc

Solute–solvent interactions in lactams–water ternary solvents†

Rafael Alcalde, Santiago Aparicio, Begoña García, María J. Dávila and José M. Leal*

Departamento de Química, Universidad de Burgos, 09001 Burgos, Spain.
E-mail: jmleal@ubu.es; Fax: +34 947 258 831; Tel: +34 947 258 819

Received (in Toulouse, France) 18th November 2004, Accepted 15th February 2005
First published as an Advance Article on the web 27th April 2005

This work reports on a variety of experiments performed as a contribution to an improved understanding of the structure and dynamics of amide-water mixtures. Several thermophysical properties of the pyrrolidin-2-one–*N*-methylpyrrolidinone–water ternary mixed solvent and its binary constituents were measured at 298.15 K. From the experimental readings excess and mixing properties were evaluated and analyzed in connection with structural effects and ternary interactions. The properties investigated support the formation of strong hydrogen bonds between water and the cyclic amides. For the binary constituents, the derived properties support 1 : 2 PYR–water and 1 : 3 NMP–water intermolecular interactions. The observed weakening of hydrogen bonds in the ternary system compared with the binary constituents reveals that no significant ternary net interactions are present in the mixture.

Introduction

Over the last decades simple liquids and non-electrolyte solvent mixtures have been characterized on the basis of their thermophysical properties. Most liquids with practical applications and/or of theoretical interest are made up of large molecules bound by weakly directional van der Waals forces and exhibit a pronounced non-ideal behaviour. Water (W), on the contrary, is made up of small molecules strongly bound by H-bonds, an order of magnitude greater than the van der Waals forces. Anomalous properties of water such as a comparatively large liquid temperature range and a large heat capacity (which drops to half upon boiling or freezing) can be explained by the density of hydrogen bonds in water. Hydrogen bonding in water is highly cooperative, that is, interaction of a water molecule with a cluster of H-bonded molecules is more likely than interaction with a single molecule to form a dimer. Therefore, pure water is arranged in a tetrahedral matrix that leads to a very stable complex network structure at low and medium temperatures.[1–3] The large density of hydrogen bonds in water enables the formation or breaking of such bonds in biomolecules with a minimum energetic cost, which confers upon biomolecules very complex structures and high reactivity at room temperature.

Amides are a very interesting class of solvents. They possess the very common—in nature—donor-acceptor CO–NH peptide bond and display the property of self-association by H-bonding. In particular, cyclic amides (lactams) are model molecules of the amide group in peptides. The *cis*-lactam pyrrolidin-2-one (PYR; also known as γ-butyrolactam) is highly self-associated in the pure state and the various types of aggregates, mainly dimers in dilute solutions ($\mu_{30\ ^\circ C}$ = 3.55 D, Scheme 1)[4,5] and higher oligomers in concentrated solutions, behave as independent entities. Therefore, PYR may serve as a model for the H-bonding of the bases in nucleic acids for more complex systems related to structural problems in molecular biology.[6] PYR is also widely used in industrial applications.[7]

On the other hand, the highly selective tertiary amide *N*-methylpyrrolidinone (NMP) is a powerful, non-protogenic, chemically stable solvent used in the extraction of aromatic compounds and in the separation of polar from non-polar compounds;[7] it has applications as a cleaning agent in the electronic industry and in coal extraction.[8] NMP is a very simple model for rigid, non-associating polar compounds and, due to its high dipole moment, is assumed to be associated by dipole–dipole interactions, the high polarity of the resulting entity ($\mu_{30\ ^\circ C}$ = 4.09 D) being attributed to formation of a favourable and stable, planar, five-membered ring. Even though hydrogen atoms attached to the nitrogen atom are lacking in this molecule, the pronounced H-bonding acceptor ability of the CO oxygen makes NMP prone to H-bonding when mixed with appropriate donor solvents.

In summary, mixed solvents containing amides are an important tool to interpret biologically interesting complex molecules. To gain a deeper insight into the structure of lactam-containing mixtures and to check the predictive ability of different theoretical models, earlier contributions on cyclic amides are extended in this work to the thermophysical properties of the PYR–NMP–W ternary system and their binary constituents.[9–12]

Experimental

The solvents PYR and NMP (Fluka), of the highest purity commercially available, were used without further purification. The solvents were degassed with ultrasound and protected from light (NMP is photosensitive) over Fluka 0.3 nm molecular sieves. Degassed ultrapure water from Millipore (Milli-Q, resistivity 18.2 mΩ cm) was used in all experiments. The purity of the solvents was determined by GC using a Perkin Elmer 990 Gas Chromatograph and by comparison with the literature thermophysical properties (Table S1 in the ESI, refs. 13–19 contained therein). The binary constituents PYR–W, NMP–W and PYR–NMP were studied at 298.15 K and atmospheric pressure over the full composition range. To avoid undesired preferential evaporation, the samples were prepared by weighing with a Mettler AT261 microbalance ($\pm 1 \times 10^{-5}$ g) and

† Electronic supplementary information (ESI) available: Thermophysical properties of pure components (Table S1), binary constituents (Tables S2, S3), ternary mixtures (Tables S4, S5), coordinates for the maxima and minima of the ternary contributions (Table S6) and coordinates for the maxima and minima of the partial molar excess properties (Table S7). See http://www.rsc.org/suppdata/nj/b4/b417601d/

DOI: 10.1039/b417601d

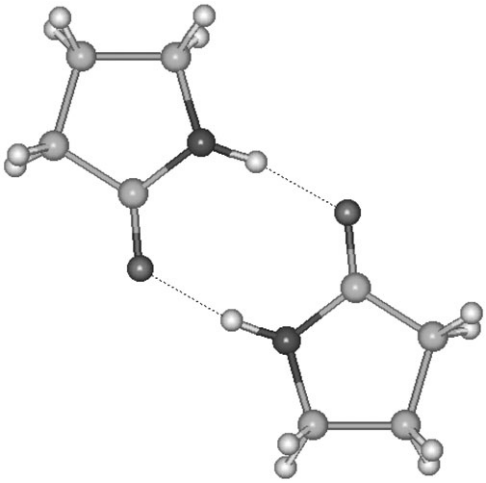

Scheme 1

syringing into vials with the same mixture volume, with a stated precision of $\pm 1 \times 10^{-4}$ mole fraction. To ensure a fair description of each of the three components, the PYR–NMP–W ternary system was studied at 298.15 K according to the sample distribution plotted in Fig. 1.

Densities (ρ) and speeds of sound (u), were measured with an Anton Paar DSA 5000 instrument. Densities were measured according to the oscillating U-tube principle ($\pm 5 \times 10^{-6}$ g cm^{-3}) and the speeds of sound by measuring the travel time through the sample of an impulse from a piezoelectric emission (± 0.5 m s^{-1}); the cell temperature was controlled by a built-in solid state thermostat ($\pm 1 \times 10^{-2}$ K). The apparatus was calibrated using water (Milli-Q) and *n*-nonane (Fluka, purity >99.5%) as reference standards.

Dynamic viscosities (η) were measured using an Anton Paar AMV200 rolling ball microviscometer whose temperature was controlled using a Julabo F25 external thermostat ($\pm 1 \times 10^{-2}$ K). The rolling time was measured to $\pm 1 \times 10^{-2}$ s with an stated precision of $\pm 5 \times 10^{-3}$ mPa s. Calibration was performed using *n*-dodecane (Aldrich, >99.5%), hexan-1-ol (Fluka, >99.5%), octan-1-ol (Fluka, >99.5%) and decan-1-ol (Fluka, >99.5%) as standards.

Refractive indexes (n_D) were measured with an automated Leica AR600 refractometer which provides a refractive index precision of $\pm 5 \times 10^{-5}$. The temperature was controlled by a Julabo F32 external circulator ($\pm 1 \times 10^{-2}$ K) and the calibration was performed using water and a standard oil (n_D = 1.51416) supplied by the manufacturer.

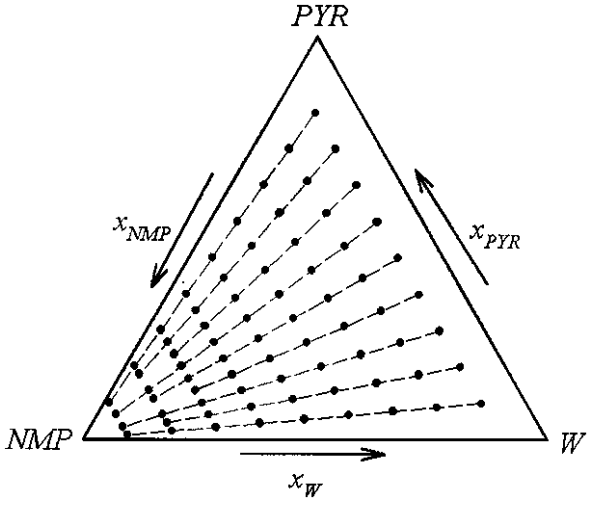

Fig. 1 Sample distribution for the study of the PYR–NMP–W ternary system.

Isobaric molar heat capacities ($C_{P,m}$) were measured using a Setaram micro DSC III calorimeter. It consists of two vessels (reference and measuring) lodged in a calorimetric block surrounded by a thermostatic liquid (*n*-undecane), which ensures a homogeneous temperature. The temperature was controlled by two type K thermocouples to $\pm 1 \times 10^{-2}$ K. The measurement principle is based on the Calvet principle, which determines the variation in the heat flow to/from the liquid sample upon temperature scanning. Measurements were performed according to the isothermal step method already described.[20] Hexane (Fluka, >99.5%) was the reference material and butan-1-ol (Aldrich, >99.5%) the calibration liquid. Heat capacities were measured to within $\pm 1 \times 10^{-2}$ J mol^{-1} K^{-1}. The experimental properties for the binary constituents and the ternary system are reported in Tables S2–S5, ESI.

Results and discussion

General remarks

Excess molar volumes (V_m^E), mixing viscosities ($\Delta_{mix}\eta$), and excess molar free energies of activation (ΔG^{*E}_m) were evaluated from the experimental readings according to the expressions reported earlier.[9–12] Isentropic compressibilities (k_S) were calculated from the Laplace equation and excess isentropic compressibilities (k_S^E) were according to the ideal behaviour criterium defined by Benson *et al.*[21] Internal pressures (P_i) and excess internal pressures (P_i^E) were calculated from the Buchler–Hirschfelder–Curtis equation of state[22] according to the procedure previously reported.[11] Excess molar isobaric heat capacities ($C_{P,m}^E$) of the binary and ternary systems were calculated according to Benson criteria.[21]

Excess thermodynamic properties reflect the non-ideal behaviour of solvents when different components are mixed and can be attributed to differences in the molecular shape and size of the components, to differences between like–like and unlike interactions, and to the reorientation of the molecules in the mixture. The excess and mixing properties for the binary constituents (X^E) were correlated with composition, x, using the Redlich–Kister eqn. (1):[23]

$$X^E = x(1-x)\sum_{j=1}^{k} A_j(2x-1) \qquad (1)$$

where x represents either the lactam mole fraction in the amide–water system or the PYR mole fraction in PYR–NMP binary compositions, the values of the A_j coefficients being obtained by a least-squares procedure and the proper number of coefficients, k, determined by an F-test.[24] The coefficients are reported in Table 1 along with the standard deviations. The ternary excess and mixing properties, X^E_{TER}, were fitted to the Cibulka[25] equation:

$$X^E_{TER} = X^E_{BIN} + x_1x_2x_3(B_0 + B_1x_1 + B_2x_2) \qquad (2)$$

where X^E_{BIN} represents the sum of the particular property for the three binary constituents deduced from eqn. (1) using the parameters of Table 1; the last term in eqn. (2) is the so-called ternary contribution to the corresponding property. The parameters deduced from a least-squares procedure are listed in Table 2 and the maxima and/or minima of the ternary contributions are given in Table S6 (ESI).

Partial molar quantities are defined as the rate of change with concentration of extensive functions and account for the binary and higher-order interactions between components. From the fitting coefficients of the molar excess volumes and molar excess heat capacities, the partial molar excess properties, $\bar{V}_m^E$ and $\bar{C}_{P,m}^E$, were evaluated for the binary constituents and the ternary system according to the intercept method,[12] the limiting values at infinite dilution being evaluated as the values at mole fraction approaching zero. Plots of the excess and

Table 1 A_i coefficients of eqn. (1) and standard deviation σ for the xPYR + (1 − x)W, xNMP + (1 − x)W and xPYR + (1 − x)NMP binary mixtures at 298.15 K.

Mixture	A_0	A_1	A_2	A_3	A_4	A_5	σ
	Excess molar volume V^E_m/cm^3 mol^{-1}						
xPYR + (1 − x)W	−2.1731	1.1070	−0.1480	−1.0170	0.9738		0.0031
xNMP + (1 − x)W	−4.4862	2.6435	−0.4154	−2.0437	2.0941		0.0084
xPYR + (1 − x)NMP	−0.8812	0.0517	−0.0286	0.0782			0.0009
	Mixing viscosity $\Delta_{mix}\eta$/mPa s						
xPYR + (1 − x)W	11.443	2.356	−11.647	4.738	2.984		0.015
xNMP + (1 − x)W	10.354	−18.403	15.742	2.949	−19.224	11.916	0.035
xPYR + (1 − x)NMP	−13.822	−6.897	−2.914	−1.632	−1.096		0.004
	Excess molar free energy of activation ΔG^{*E}_m/kJ mol^{-1}						
xPYR + (1 − x)W	12.823	−7.679	3.170	−0.676			0.002
xNMP + (1 − x)W	14.313	−14.811	9.308	−4.749	3.071		0.022
xPYR + (1 − x)NMP	−1.527	−0.266	−0.072	−0.017			0.002
	Excess isentropic compressibility k^E_S/TPa^{-1}						
xPYR + (1 − x)W	−193.32	245.77	−190.80	135.63	−232.29	182.58	0.35
xNMP + (1 − x)W	−273.25	353.30	−266.06	203.86	−383.87	303.57	0.53
xPYR + (1 − x)NMP	−32.85	1.09	−4.18				0.05
	Excess internal pressure P^E_i/MPa						
xPYR + (1 − x)W	−271.27	119.76	−67.11	41.35			0.41
xNMP + (1 − x)W	−351.40	183.14	−87.99	84.59	−67.55		0.23
xPYR + (1 − x)NMP	−4.72	−0.57	−0.09				0.00
	Excess isobaric molar heat capacity $C^E_{P,m}$/J mol^{-1}						
xPYR + (1 − x)W	30.52	−23.07	5.59	−2.41	16.78		0.11
xNMP + (1 − x)W	39.12	−42.20	27.24				0.22
xPYR + (1 − x)NMP	1.81	−0.12	1.08	−0.03			0.01

mixing properties for the ternary and binary systems are reported in Figs. 2–14 and discussed in more detail below; to provide an easier view of the ternary system, projections of the level curves for the three-dimensional plots are also provided.

The lactam–W binary constituents

The structures of PYR and W are governed by H-bonding, whereas NMP displays strong dipole–dipole interactions. The excess and mixing properties (Figs. 2–5) show a pronounced non-ideal behaviour; excess molar volumes were remarkably negative for the two lactam–W systems with a greater contraction for NMP–W, the minima being −0.5738 cm^3 mol^{-1} at x_{PYR} = 0.3988 for PYR–W and −1.2041 cm^3 mol^{-1} at x_{NMP} = 0.3868 for NMP–W. These contraction effects can be attributed to two main factors: (i) the strong lactam–water intermolecular forces and (ii) the very different shape and size of the lactams compared to water, which gives rise to noticeable geometry effects. The greater values for NMP–W arise from the weaker association forces in pure NMP (with a subsequent strong mixing effect) compared to pure PYR, which is self-aggregated in the pure state.

The partial molar excess volumes (Fig. 4) of the three components show a complex behaviour; Table S7 (ESI) gives

Table 2 B_i coefficients of eqn. (2) and standard deviation σ for the x_1PYR + x_2NMP + (1 − x_1 − x_2)W ternary mixtures at 298.15 K.

Property	B_0	B_1	B_2	σ
$V^E_{m,TER}$/cm^3 mol^{-1}	4.0514	−1.9194	−2.6627	0.0303
$\Delta_{mix}\eta_{TER}$/mPa s	13.072	−86.406	1.568	0.7416
$\Delta G^{*E}_{m,TER}$/kJ mol^{-1}	−47.325	28.222	72.846	0.266
$k^E_{S,TER}$/TPa^{-1}	−709.77	622.14	1162.70	7.217
$P^E_{i,TER}$/MPa	583.25	−477.49	−540.99	6.553
$C^E_{P,m,TER}$/J mol^{-1}	15.56	21.55	46.64	0.99

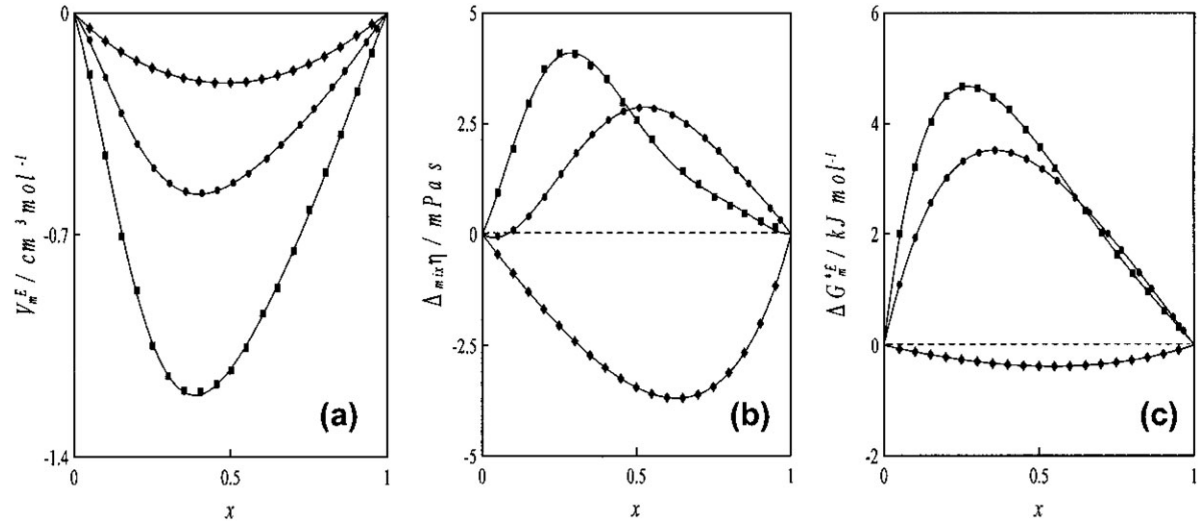

Fig. 2 (a) Molar excess volume, V_m^E, (b) mixing viscosity, $\Delta_{mix}\eta$, and (c) molar excess Gibbs energy of activation, ΔG^{*E}_m, of the (●) *x*PYR + (1 − *x*)W, (■) *x*NMP + (1 − *x*)W and (◆) *x*PYR + (1 − *x*)NMP binary mixtures at 298.15 K.

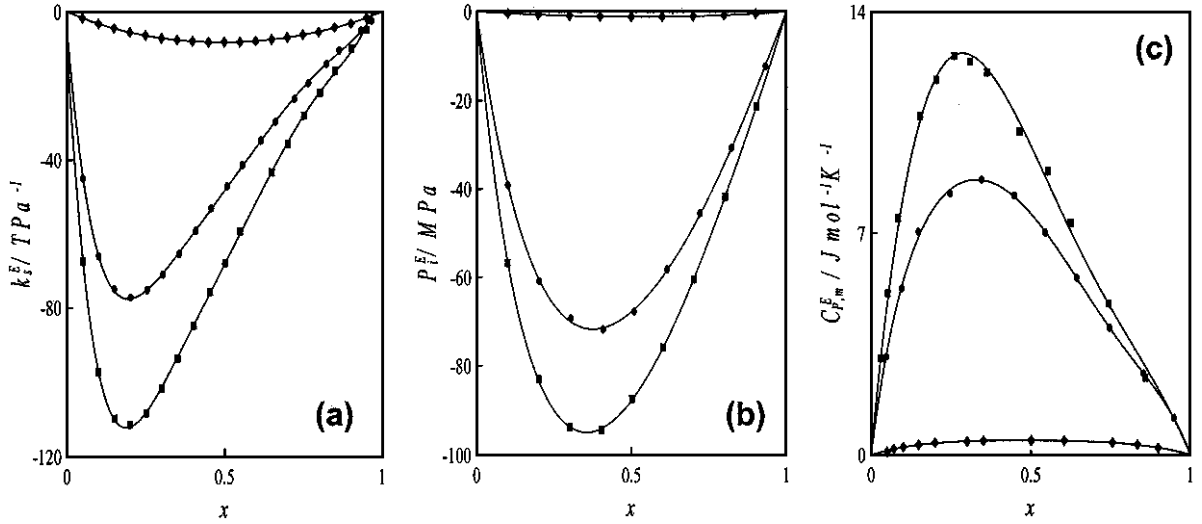

Fig. 3 (a) Excess isentropic compressibility, k_S^E, (b) excess internal pressure, P_i^E, and (c) molar excess isobaric heat capacity, $C_{P,m}^E$, of the (●) *x*PYR + (1 − *x*)W, (■) *x*NMP + (1 − *x*)W and (◆) *x*PYR + (1 − *x*)NMP binary mixtures at 298.15 K.

the maxima, minima and infinite dilution values. The lactam partial molar excess volumes [Fig. 4(a) and 4(b)] display two strong minima at low lactam concentration (greater for NMP); at high lactam concentration, however, an inversion with a smooth maximum for NMP occurs. The W partial molar excess volumes [Fig. 4(b)] show a similar behaviour, though the shapes were somewhat more complex; for both lactam–W systems a minimum appears at high lactam concentration, greater for NMP; at low lactam concentration an inversion occurs with a soft maximum for NMP–W (Fig. 4). Table S7 (ESI) collects the location of the minima for the lactam partial

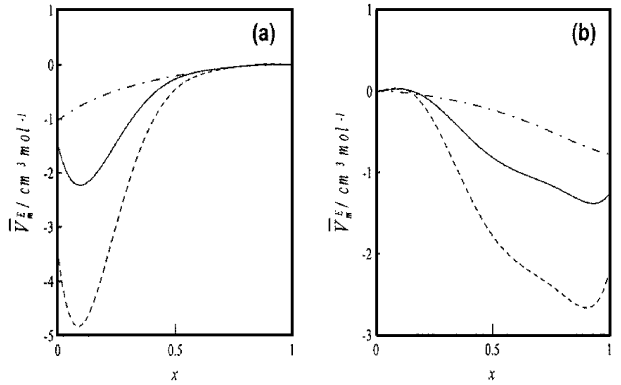

Fig. 4 Partial molar excess volumes, $\bar{V}_m^E$, of (a) lactam, in lactam + water mixtures, or PYR, in PYR + NMP mixtures, and (b) water, in lactam + water mixtures, or NMP, in PYR + NMP mixtures for the (—) *x*PYR + (1 − *x*)W, (---) *x*NMP + (1 − *x*)W and (– · –) *x*PYR + (1 − *x*)NMP binary mixtures at 298.15 K.

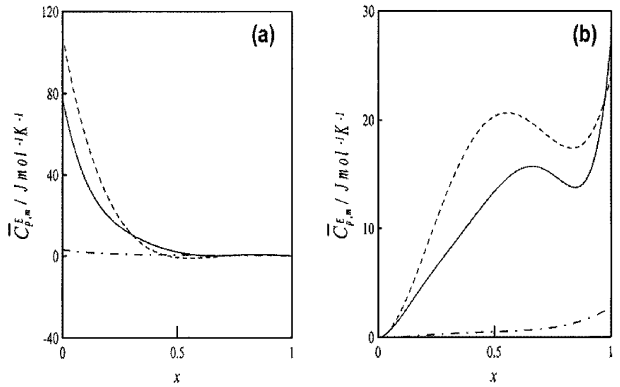

Fig. 5 Partial molar excess isobaric heat capacities of both components, $\bar{C}_{P,m}^E$, for the (—) *x*PYR + (1 − *x*)W, (---) *x*NMP + (1 − *x*)W and (– · –) *x*PYR + (1 − *x*)NMP binary mixtures at 298.15 K.

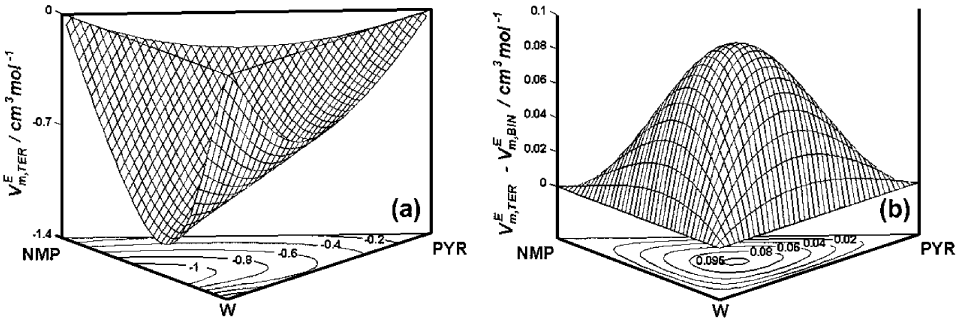

Fig. 6 (a) Molar excess volume, $V^{E}_{m,TER}$, and (b) ternary contribution of molar excess volume, $V^{E}_{m,TER} - V^{E}_{m,BIN}$, of the x_1PYR + x_2NMP + $(1 - x_1 - x_2)$W ternary mixtures at 298.15 K.

molar excess volume, and the maxima for the W partial molar excess volumes at the same composition, showing the opposite contributions of W and the lactams to the volumetric properties.

Partial molar volumes at infinite dilution, $\bar{V}^{E,\infty}_{m,i}$, are very important properties because they take into account both geometric factors and solute-solvent interactions. This property can be split into different contributions according to eqn. (3):[26,27]

$$\bar{V}^{E,\infty}_{m,i} = V_{W,i} + V_{e,i} - V_i \quad (3)$$

where $V_{W,i}$ is the intrinsic solute van der Waals volume, $V_{e,i}$ is the free volume, and V_i the solute molar volume. The van der Waals term represents the inaccessible volume for the solvent (Table 3); the free volume is a measure of the solute-solvent interstitial volume and accounts for all solute-solvent interaction effects.[27] Substitution of the lactams' infinite dilution values (Table S7, ESI) into eqn. (3) affords the free volumes $V_{e,PYR}$ = 24.91 cm^3 mol^{-1} and $V_{e,NMP}$ = 32.64 cm^3 mol^{-1}, that is, the higher the van der Waals volume (*i.e.*, for NMP) the larger the free volume. On the basis of the W partial molar excess volume at infinite dilution, W free volumes of 4.29 cm^3 mol^{-1} in PYR and 3.46 cm^3 mol^{-1} in NMP were deduced, the PYR excluded volume being greater due to its dimer structure.

On the basis of the volumetric properties, application of the scaled particle theory (SPT)[30] to partial molar excess volumes at infinite dilution provides further information into the structure of these systems; according to this model the limiting partial molar excess volume of a solute *i* can be split into the terms:

$$\bar{V}^{E,\infty}_{m,i} = V_c + V_{int} + k_T RT - V_i \quad (4)$$

where V_c and V_{int} represent the cavity formation and solute-solvent interaction contributions, respectively. According to the SPT model the transfer of a solute from a gas to a liquid can be envisaged in two steps:[27,32,33] (i) formation of a solvent cavity with the result of the V_c expansion and (ii) due to an attraction effect the solute-solvent interactions give rise to the V_{int} contraction contribution. The V_{int} values were determined by combining the limiting partial molar excess volumes and the V_c values (Table 4), the latter being evaluated with eqns. (5)

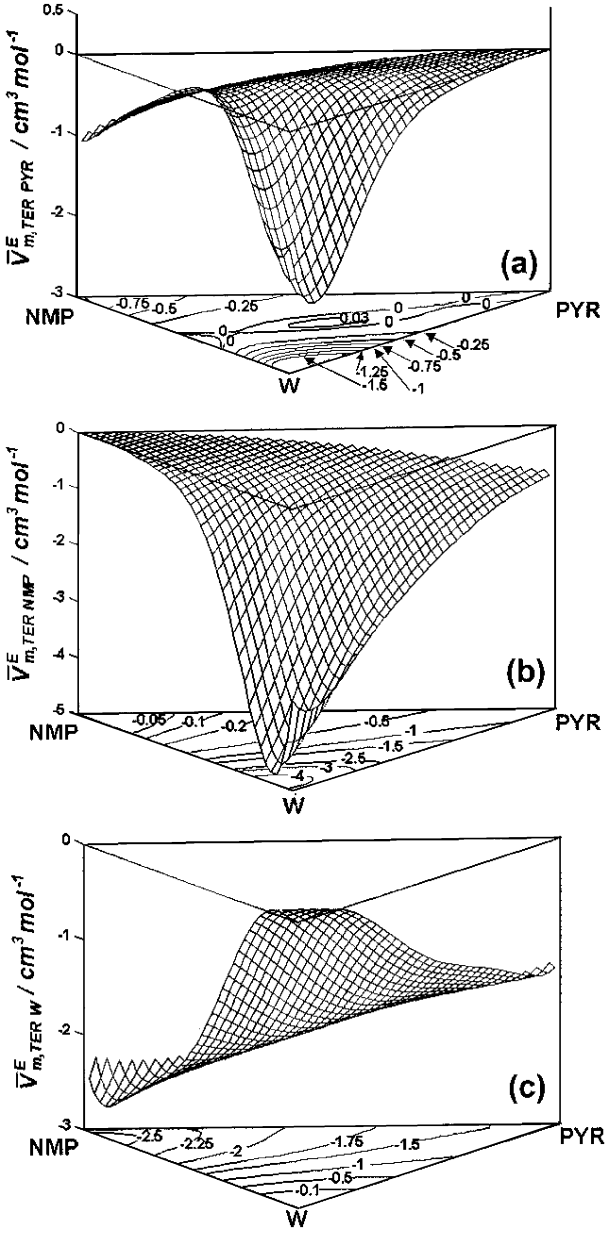

Fig. 7 Partial molar excess volumes of component *i*, $\bar{V}^{E}_{m,TER,i}$, for the x_1PYR + x_2NMP + $(1 - x_1 - x_2)$W ternary mixtures at 298.15 K.

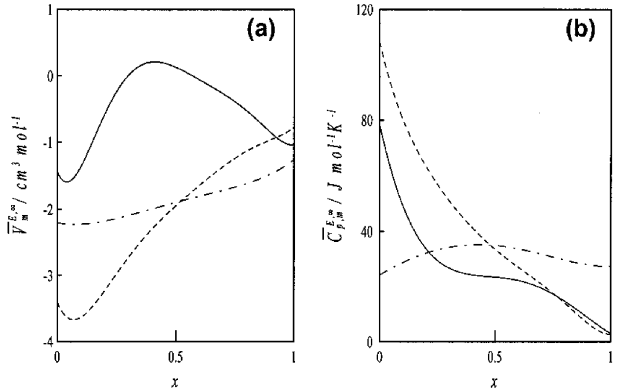

Fig. 8 (a) Infinite dilution partial molar excess volumes, $\bar{V}^{E,\infty}_{m}$, and (b) infinite dilution partial molar excess isobaric heat capacities, $\bar{C}^{E,\infty}_{P,m}$, for the x_1PYR + x_2NMP + $(1 - x_1 - x_2)$W ternary mixtures at 298.15 K. Properties for: (—) PYR as a function of *x*NMP + $(1 - x)$W (x_{PYR} = 0); (---) NMP as a function of *x*PYR + $(1 - x)$W (x_{NMP} = 0); (– · –) W as a function of *x*PYR + $(1 - x)$NMP (x_W = 0).

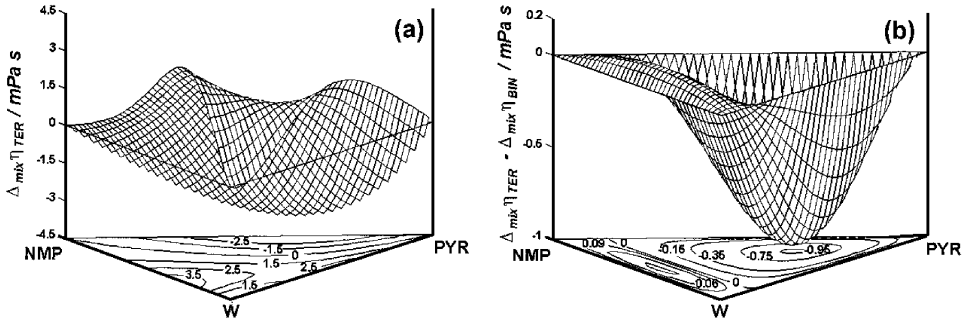

Fig. 9 (a) Mixing viscosity, $\Delta_{\mathrm{mix}}\eta_{\mathrm{TER}}$, and (b) ternary contribution of mixing viscosity, $\Delta_{\mathrm{mix}}\eta_{\mathrm{TER}} - \Delta_{\mathrm{mix}}\eta_{\mathrm{BIN}}$, of the x_1PYR + x_2NMP + $(1 - x_1 - x_2)$W ternary mixtures at 298.15 K.

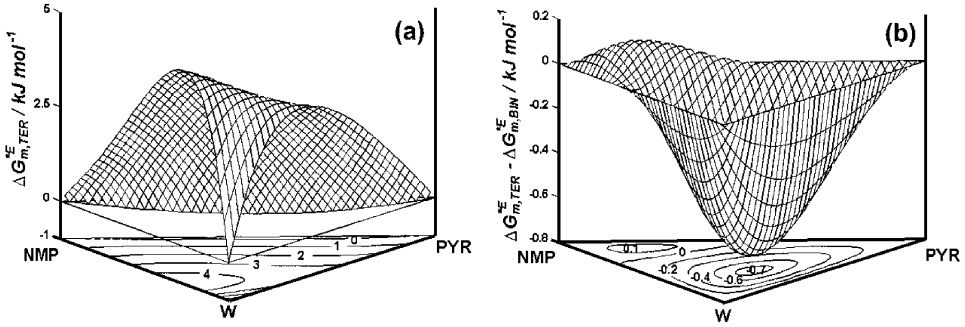

Fig. 10 (a) Molar excess Gibbs energies of activation, $\Delta G^{*\mathrm{E}}_{\mathrm{m,TER}}$, and (b) ternary contribution of molar excess Gibbs energies of activation, $\Delta G^{*\mathrm{E}}_{\mathrm{m,TER}} - \Delta G^{*\mathrm{E}}_{\mathrm{m,BIN}}$, of the x_1PYR + x_2NMP + $(1 - x_1 - x_2)$W ternary mixtures at 298.15 K.

and (6):

$$V_{\mathrm{c}} = k_{T,1}RT(1-y)^{-3} \times \left((1-y)^2 + \frac{3(1-y)\sigma_2}{\sigma_1} + 3(1+2y)\left(\frac{\sigma_2}{\sigma_1}\right)^2\right) \quad (5)$$

$$y = \frac{\pi N_{\mathrm{A}}\sigma_1^3}{6V_1} \quad (6)$$

where subscripts 1 and 2 refer to solvent and solute, respectively, and σ_i represents the hard sphere radii calculated from the vaporization enthalpies (Table 3).

The NMP cavity volume in water is greater than that of PYR because of the relative shapes and sizes, but the interaction volume (absolute value) is greater for PYR. The –NH–CO– group possesses one hydrogen-bond donor (the hydrogen atom) and three acceptors (two lone pair of electrons on oxygen and one on nitrogen) and PYR thus can participate in an efficient PYR–W H-bonding interaction,[34] giving rise to a greater V_{int} value; however, NMP can only form hydrogen bonds through the CO oxygen because there are no hydrogen atoms on the N atom and the methyl group hinders the amide nitrogen. Stepwise dilution of W in the lactams is followed by increasing the PYR cavity and interaction volumes, as expected from the PYR–PYR dimers. Likewise, the component with lowest isothermal compressibility, PYR (Table 3), yields a greater interaction volume whereas NMP, with a lower internal pressure (Table S1, ESI), gives a lower cavity volume.[35] Therefore, the cavity volume is the main factor contributing to the infinite dilution properties of the lactam–W systems, consistent with the difference in size of the mixing molecules.

Further information may be deduced from the other properties measured. Viscosity is an important transport property of liquids, either pure or mixed. The force needed to make a fluid layer move in relation to a neighbouring layer is called shear; hence shear viscosity reflects the internal friction of a fluid and provides a measure of the extent of the interactions. Mixing viscosities and molar excess free energies of activation for the two lactam–W systems were positive [Fig. 2(b) and 2(c)] and larger for NMP–W, this feature also denoting an efficient and strong lactam–W H-bonding.[36] The maxima of mixing viscosities were 2.876 mPa s at $x_{\mathrm{PYR}} = 0.5258$ (1 : 2 PYR : W) and 4.099 mPa s at $x_{\mathrm{NMP}} = 0.2815$ (1 : 3 NMP : W). This noticeable difference appears because pure NMP is not H-bonded and further mixing with W causes this interaction, with the resulting high increase in viscosity; pure PYR, on the contrary, is strongly self-associated and mixing with W does not produce

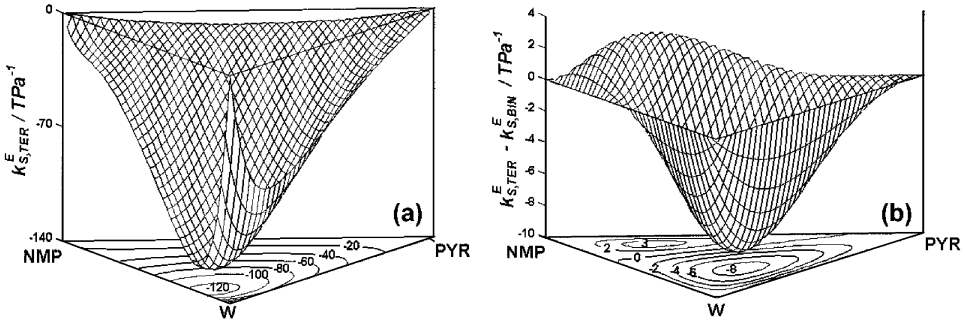

Fig. 11 (a) Excess isentropic compressibility, $k^{\mathrm{E}}_{\mathrm{S,TER}}$, and (b) ternary contribution of excess isentropic compressibility, $k^{\mathrm{E}}_{\mathrm{S,TER}} - k^{\mathrm{E}}_{\mathrm{S,BIN}}$, of the x_1PYR + x_2NMP + $(1 - x_1 - x_2)$W ternary mixtures at 298.15 K.

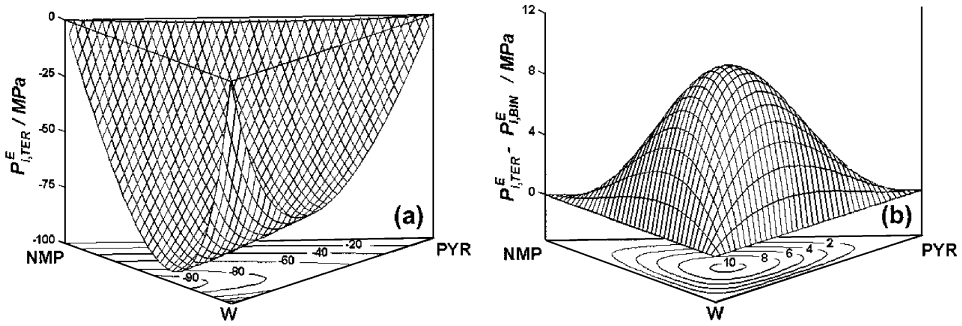

Fig. 12 (a) Excess internal pressure, $P^{E}_{i,TER}$, and (b) ternary contribution of excess internal pressure, $P^{E}_{i,TER} - P^{E}_{i,BIN}$, of the x_1PYR + x_2NMP + $(1 - x_1 - x_2)$W ternary mixtures at 298.15 K.

such a strong viscosity effect. The maximum at equimolar PYR–W composition indicates that the cyclic lactam structure is retained up to about $x = 0.5$, where W starts to work as solvent. The strong maximum for NMP–W at low lactam concentration (1 : 3) indicates a very effective interaction between unlike molecules. If the lactam concentration increases then this interaction becomes less effective because the NMP–NMP dipole interactions are a barrier for H-bonding over this concentration range; it should be noted that mixing viscosities for NMP were greater than for PYR at low amide concentrations, but at high amide concentration the ordering changed, consistent with the SPT results.

Several authors have suggested that excess isentropic compressibilities become increasingly negative with an increase in the strength of unlike interactions.[37,38] Excess isentropic compressibilities showed strong minima, -77.33 TPa^{-1} at $x_{PYR} = 0.1931$ for PYR and -112.03 TPa^{-1} at $x_{NMP} = 0.1848$ for NMP [Fig. 3(a)], revealing the existence of strong lactam–W H-bonding. The deeper minimum for the latter can also be attributed to the absence of H-bonds in pure NMP; at low amide concentration NMP causes a disruption of the W structure (also confirmed by the larger cavity volume from SPT analysis), thus slowing the compressibility down to a deeper minimum.

Internal pressure, defined as the energy required to vaporize a unit volume of a substance, is closely related to the cohesive energy density and provides a measure of the strength of interactions. The internal pressure, P_i, involves the fundamental parameters (polarity and structure) associated with the behaviour of liquid mixtures and, in contrast to excess properties, provides values different from zero for the pure components. An analysis of the excess internal pressure [Fig. 3(b)] leads to similar conclusions; this property is strongly negative for the two systems, with minima of -71.73 MPa at $x_{PYR} = 0.3767$ for PYR and -94.90 MPa at $x_{NMP} = 0.3552$ for NMP. The greater PYR internal pressure relative to NMP (Table S1, ESI) reveals the stronger H-bonding structure of pure PYR compared with the dipolar structure of pure NMP. The negative excess internal pressure emerging upon mixing with W indicates the formation of PYR–W H-bonds; the less negative values for PYR–W reflect the residual PYR–PYR self associations remaining in the mixture that lead to a smaller internal pressure as compared with NMP.

The high isobaric molar heat capacities deduced (Figs. 3 and 5 and Table S1, ESI) indicate strong intermolecular forces for the two systems. The excess isobaric molar heat capacities, ($C^{E}_{P,m}$) for the water-containing mixtures, large and positive, gave maxima of 8.70 J mol^{-1} K^{-1} at $x_{PYR} = 0.3295$ for PYR and 12.70 J mol^{-1} K^{-1} at $x_{NMP} = 0.2852$ for NMP; these positive values indicate the existence of strong H-bonding heteroassociations, the values for PYR being smaller because of the residual PYR–PYR interactions that remain after mixing. The partial molar excess isobaric heat capacities, $\bar{C}^{E}_{P,m}$, are plotted in Fig. 5; Table S7 (ESI) collects the maxima and minima along with the values at infinite dilution. The behaviour of the lactams' partial molar excess isobaric heat capacities is complex and shows a sharp decrease with an increase in lactam concentration and maxima at high amide concentration. In the W-rich region the $\bar{C}^{E}_{P,m}$ values were higher for NMP–W and in the lactam rich region an inversion results, concurrent with the partial molar excess volumes (Fig. 4). The infinite dilution values reveal strong W–lactam interactions (Table S7, ESI), the small maxima at high amide concentration and the larger value for PYR being attributed to the lactam dimers. The water partial molar excess isobaric heat capacities, smaller than those of the lactams, are also complex and show maxima and minima and an ordering inversion in the lactam-rich ranges.

The properties analyzed support strong lactam–W H-bonding. The existence of weaker intermolecular forces in pure NMP affords stronger mixing properties; the residual PYR–PYR interactions in the PYR mixtures and the different degrees of association between both molecules and water may be the reason for the different behaviour of the two systems.

The PYR–NMP binary constituent

The excess and mixing properties of the PYR–NMP binary constituent (Figs. 2–5) are smaller and display a simpler

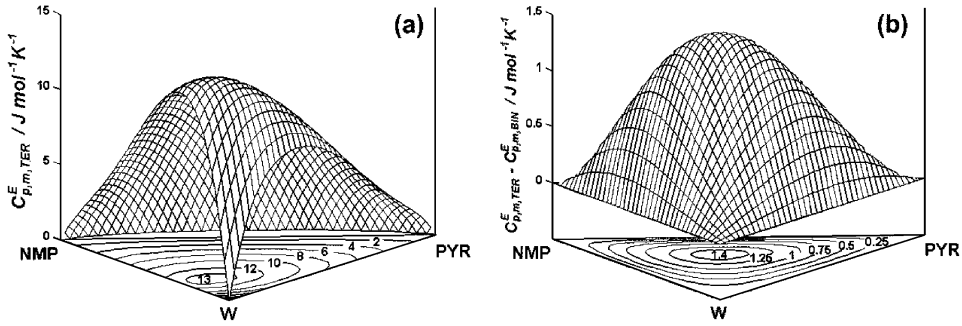

Fig. 13 (a) Molar excess isobaric heat capacity, $C^{E}_{P,m,TER}$, and (b) ternary contribution of molar excess isobaric heat capacity, $C^{E}_{P,m,TER} - C^{E}_{P,m,BIN}$, of the x_1 PYR + x_2NMP + $(1 - x_1 - x_2)$W ternary mixtures at 298.15 K.

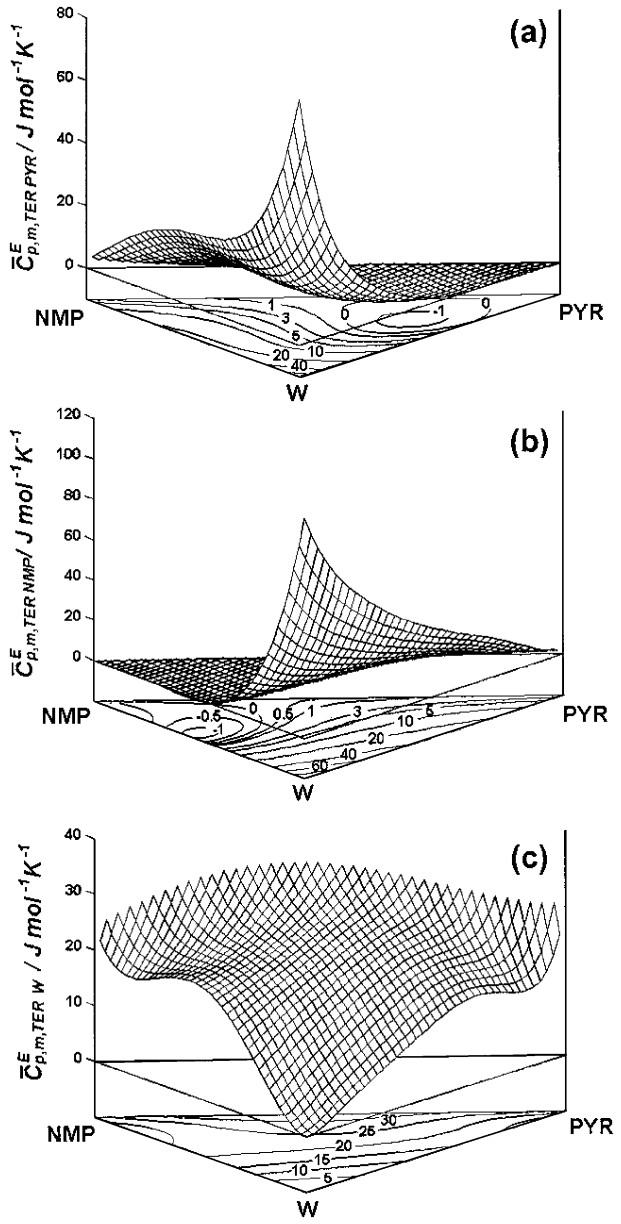

Fig. 14 Partial molar excess isobaric heat capacities of (a) PYR, (b) NMP and (c) W, $\bar{C}^{E}_{P,m,TER,i}$, for the x_1PYR + x_2NMP + (1 − x_1 − x_2)W ternary mixtures at 298.15 K.

behaviour. The molar excess volume is slightly negative, with a minimum of −0.2205 cm^3 mol^{-1} at x_{PYR} = 0.4848 caused by the very efficient packing due to the similar shape of both molecules. The partial molar excess volumes (Fig. 4) show a regular trend without maxima or minima; the infinite dilution values listed in Table S7 (ESI) are smaller for NMP due to its larger size and the dimer nature of PYR that produces a less efficient packing; in contrast, PYR molecules may be packed more tightly in the less compact NMP structure. The infinite dilution values afford the free volumes $V_{e,PYR}$ = 25.31 cm^3 mol^{-1} and $V_{e,NMP}$ = 35.26 cm^3 mol^{-1}, the greater NMP free volume giving rise to a smaller partial molar excess volume at infinite dilution; therefore, geometric factors, mainly size, determine the values of this property.

Application of the SPT model to NMP and PYR affords a larger cavity volume for NMP, consistent with its shape requirements for a greater cavity when dissolved in PYR than for PYR dissolved in NMP (Table 4). Also, NMP gives a greater interaction volume because the cyclic PYR–PYR dimers are a barrier for the interaction with NMP molecules; however, when PYR is dissolved in NMP an interaction appears because NMP is not H-bonded while PYR has two hydrogen bonding sites.

Mixing viscosities (Fig. 2) are negative, with a pronounced minimum of −3.694 mPa s at x_{PYR} = 0.6298, which eliminates the existence of H-bonding between both lactams. The PYR–PYR interactions are disrupted by the presence of NMP, an effect not balanced by new heteroassociations. This feature is confirmed by the negative ΔG^{*E}_m and the close to zero k^E_S, P^E_i and $C^E_{P,m}$ values (Figs. 2 and 3). The partial molar excess isobaric heat capacities (Fig. 5) show a regular trend, with small infinite dilution values similar for both lactams (Table S7, ESI).

In summary, the mixing process for the NMP–PYR constituent is controlled by geometric factors and the efficient packing favoured by the shapes of both molecules, but with a disruption of the like–like interactions not balanced by the formation of new interactions.

The PYR–NMP–W ternary system

The behaviour of the binary constituents of this system is very complex and therefore the structure of the ternary mixture should, in principle, be even more complex. The excess molar volume [Fig. 6(a)] was negative over the whole composition range; the greater values that appear in the water-rich zones reflect, although geometry effects are important, that the main contributing factor is the lactams–water H-bonding. The ternary contribution [Fig. 6(b)] is always positive but not too high, with a maximum at 1PYR : 1NMP : 2W (Table S6, ESI). Although the small ternary contributions would indicate that the simultaneous presence of three molecules does not notably affect either the like–like or the unlike binary interactions, the formation of this maximum does not support ternary associations and denotes that the molar excess volume is controlled mainly by geometric factors.

The partial molar excess volumes are negative for the three molecules, except for PYR in lactam-rich regions (Fig. 7), and show a very complex behaviour. The values for the lactams are more negative in the water-rich areas near the infinite dilution limit and for water in both lactam-rich zones, denoting strong lactam–W interactions; the simultaneous presence of both lactams diminishes this property. The infinite dilution values are plotted in Fig. 8; upon dissolving PYR in the NMP–W binary solvent (continuous line) the values become less negative with an increase in the NMP content, giving rise to a maximum; this feature reveals a competition between NMP and PYR to bind water at the PYR infinite dilution limit. A similar trend appears for NMP (dashed line) with increasing values when the PYR content increases. For W (dashed–dot line) the property is less negative when PYR concentration

Table 3 Isobaric thermal expansivity, α_P, isothermal compressibility, k_T, molar volume, V_i, van der Waals volume, $V_{W,i}$, standard vaporization enthalpy, ΔH^o_V, and hard sphere diameter, σ, at 298.15 K

Component	α_P/kK^{-1}	k_T/TPa^{-1}	V_i/cm^3 mol^{-1}	$V_{W,i}$/cm^3 mol^{-1}	ΔH^o_V/kJ mol^{-1}	σ/Å
PYR	0.726[a]	413.79[d]	76.85[e]	50.5[f]	68.7[g]	5.41[h]
NMP	0.850[b]	526.68[d]	96.44[e]	60.4[f]	49.72[b]	5.68[h]
W	0.257[c]	452.85[d]	18.07[e]	12.4[f]	43.99[c]	2.75[i]

[a] Ref. 13. [b] Ref. 7. [c] Ref. 16. [d] Calculated from α_p, k_S and $C_{P,m}$ (Table S1, ESI). [e] Calculated from density values (Table S1, ESI). [f] Ref. 28. [g] Ref. 29. [h] Calculated using α and ΔH^o_V according to the procedure of Pierotti. [30] [i] Ref. 31.

Table 4 Cavity volume, V_c, and interaction volume, V_{int}, from SPT theory for the solutes and mixtures considered at 298.15 K

Solvent	Solute	V_c/cm^3 mol^{-1}	V_{int}/cm^3 mol^{-1}	y
W	PYR	88.06	−13.77	0.363
PYR	W	44.38	−28.72	0.650
W	NMP	99.44	−7.52	0.363
NMP	W	34.36	−19.80	0.599
NMP	PYR	138.49	−63.98	0.599
PYR	NMP	194.72	−100.09	0.650

increases, as foreseen from the behaviour of the binary constituents.

Mixing viscosities [Fig. 9(a)] are positive in the water-rich zones and negative when both lactams are prevailing. The ternary contributions [Fig. 9(b)] are predominantly negative and the minimum at (roughly) 2PYR : 1NMP : 1W eliminates ternary heteroassociations (Table S6, ESI). Because of the absence of lactam–lactam heteroassociations this is the least favourable composition for H-bonding; on the contrary, the maximum of the ternary contribution appears when water and one of the two lactams are predominant. These results are supported also by the behaviour of the excess molar Gibbs energy of activation and its ternary contribution (Fig. 10).

The excess isentropic compressibilities [Fig. 11(a)] are always negative, with less negative values when the water content decreases. The ternary contribution [Fig. 11(b)] shows a maximum in the water-poor regions and a minimum in water-rich regions (Table S6, ESI), this feature indicating that the presence of the three components is not followed by ternary interactions and that water controls the formation of H-bonds with both lactams.

Internal pressures [Fig. 12(a)] are always negative and move sharply to less negative values when the water content decreases. The ternary contribution [Fig. 12(b)] is always positive with a maximum at (roughly) 1PYR : 1NMP : 2W (Table S6, ESI); therefore, geometric factors arising from the shape and size of the molecules involved appear as the main factors in the ternary system.

Excess molar isobaric heat capacities and the ternary contributions (Fig. 13) are always positive, consistent with the sign of the ternary contribution to the excess molar volume. The slight expansion compared with the binary constituents affords a positive ternary contribution to the heat capacity, although no ternary heteroassociations were observed. The partial molar excess isobaric heat capacities (Fig. 14) and the infinite dilution values are strongly positive (Fig. 8). The lactam values increase with the water content and the water values are smaller when both lactams are simultaneously present. The same behaviour is reported for the values at infinite dilution, thus confirming the aforementioned conclusions.

Concluding remarks

The binary constituents and the ternary system display a complex behaviour, determined by the shape and size of the three components and the water–lactam H-bonding. Water interacts more efficiently with PYR because of the two bonding sites available in PYR, while a strong mixing effect appears in NMP, due to absence of H-bonds in pure NMP. The PYR–NMP binary system exhibits no unlike H-bonding, but rather an efficient packing between both molecules in the mixture followed by strong disruption of like-like interactions.

For the PYR–NMP–W ternary system the behaviour of the properties eliminates the formation of ternary associations; the binary interactions between each lactam and water remain in the ternary mixture, although they are weakened or even destroyed when the water concentration decreases and the lactam concentrations increase.

Acknowledgements

The financial support by Junta de Castilla y León, Project BU10/03, and Ministerio de Ciencia y Tecnología, project PPQ2002-02150, Spain, is gratefully acknowledged.

References

1 A. K. Soper, F. Bruni and M. A. Ricci, *J. Chem. Phys.*, 1997, **106**, 247.
2 P. G. Kusalik and F. H. Stillinger, *Science*, 1994, **265**, 1219.
3 G. Sutmann and R. Vallauri, *J. Mol. Liq.*, 2002, **98–99**, 213.
4 E. Dachwitz and M. Stockhausen, *Ber. Bunsenges. Phys. Chem.*, 1987, **91**, 1347.
5 N. A. Prokopenko, I. A. Bethea, C. J. Clemens, A. Klimek, K. Wargo, C. Spivey, K. Waziri and A. Grushow, *Phys. Chem. Chem. Phys.*, 2002, **4**, 490.
6 S. K. Mehta and R. K. Chauhan, *Fluid Phase Equilib.*, 2001, **187–188**, 209.
7 G. Hradetzky, I. Hammerl, H. J. Bittrich, K. Wehner and W. Kisan, *Selective Solvents*, Physical Sciences Data 31, Elsevier, Amsterdam, 1989.
8 C. C. Giri and D. K. Sharma, *Fuel*, 2000, **79**, 577.
9 B. García, S. Aparicio, R. Alcalde, M. J. Dávila and J. M. Leal, *Ind. Eng. Chem. Res.*, 2004, **43**, 3205.
10 B. García, R. Alcalde, S. Aparicio, J. L. Trenzado and J. M. Leal, *Ind. Eng. Chem. Res.*, 2003, **42**, 920.
11 B. García, R. Alcalde, S. Aparicio and J. M. Leal, *Phys. Chem. Chem. Phys.*, 2002, **4**, 1170.
12 B. García, R. Alcalde, J. M. Leal and J. S. Matos, *J. Phys. Chem. B*, 1997, **101**, 7991.
13 B. García, F. J. Hoyuelos, R. Alcalde and J. M. Leal, *Can. J. Chem.*, 1996, **74**, 121.
14 P. L. Pirilä-Honkanen and P. A. Roustesuo, *J. Chem. Eng. Data*, 1987, **32**, 303.
15 P. Assarsson and F. R. Eirich, *J. Phys. Chem.*, 1968, **72**, 2710.
16 J. A. Riddick, W. B. Bunger and T. K. Sakano, *Organic Solvents, Techniques of Chemistry*, Wiley, New York, 1986.
17 *Handbook of Chemistry and Physics*, ed. D. R. Lide, CRC Press, Boca Raton, 82nd edn., 2001.
18 R. P. Sing, C. P. Sinha, J. C. Das and P. Ghosh, *J. Chem. Eng. Data*, 1990, **35**, 93.
19 E. W. Lemmon, M. O. McLinden and D. G. Friend, *Thermophysical Properties of Fluid Systems*, NIST Chemistry WebBook, NIST Standard Reference Database Number 69, eds. P. J. Linstrom and W. G. Mallard, National Institute of Standards and Technology, Gaithersburg MD, March 2003, 20899 (http://webbook.nist.gov).
20 C. A. Cerdeiriña, J. A. Migues, E. Carballo, C. A. Tovar, E. de la Puente and L. Romaní, *Thermochim. Acta*, 2000, **347**, 37.
21 G. C. Benson and O. Kiyohara, *J. Chem. Thermodyn.*, 1979, **11**, 1061.
22 J. O. Hirschfelder, C. F. Curtis and R. B. Bird, *Molecular Theory of Gases and Liquids*, Wiley, New York, 1964.
23 O. Redlich and T. Kister, *Ind. Eng. Chem.*, 1948, **40**, 345.
24 P. Bevington, *Data Reduction and Error Analysis for the Physical Sciences*, McGraw-Hill, New York, 1969.
25 I. Cibulka, *Collect. Czech. Commun.*, 1982, **47**, 1414.
26 S. Teresawa, H. Itkusi and S. Arakawa, *J. Phys. Chem.*, 1975, **79**, 2345.
27 L. Lepori, E. Matteoli, A. Spanedda, C. Duce and M. R. Tiné, *Fluid Phase Equilib.*, 2002, **201**, 119.
28 Y. Marcus, *The Properties of Solvents*, John Wiley and Sons, New York, 1999.
29 W. V. Steele, R. D. Chirico, A. Nguyen, L. A. Hossenlopp and N. K. Smith, *AIChE Symp. Ser.*, 1989, **85**, 140.
30 R. A. Pierotti, *Chem. Rev.*, 1976, **76**, 717.
31 R. A. Pierotti, *J. Phys. Chem.*, 1965, **69**, 281.
32 L. Bernazzani, V. Mollica and M. R. Tiné, *Fluid Phase Equilib.*, 2002, **203**, 15.
33 B. Lee, *Biophys. Chem.*, 1994, **51**, 271.
34 G. Graziano, *Can. J. Chem.*, 2001, **79**, 1310.
35 D. Rudan-Tasic and C. Klofutar, *Monatsh. Chem.*, 1998, **129**, 1245.
36 R. Fort and W. R. Moore, *Trans. Faraday. Soc.*, 1966, **62**, 1112.
37 R. Fort and W. R. Moore, *Trans. Faraday Soc.*, 1965, **61**, 2102.
38 O. Kiyohara and K. Arakawa, *Bull. Chem. Soc. Jpn.*, 1971, **44**, 1230.